applied sciences

MDPI

Article

Metabolism, Organ Distribution, and Blood-Brain Barrier Penetration of Human Milk Oligosaccharides—6′/3′-Sialyl-*N*-acetyllactosamine

Runmiao Jiao [1,2,3,†], Eryi Ju [2,3,†], Jianjun Li [2], Zhuo A. Wang [2], Bowen Jiang [1,2,3], Mengyuan Zhao [2], Bing Wang [4], Eika W. Qian [1,*] and Yuguang Du [2,*]

1 Graduate School of Bio-Applications and Systems Engineering, Tokyo University of Agriculture and Technology, Nakacho 2-24-16, Koganei 184-8588, Tokyo, Japan; jiaorunmiao2017@163.com (R.J.); s208353x@st.go.tuat.ac.jp (B.J.)
2 State Key Laboratory of Biopharmaceutical Preparation and Delivery, Institute of Process Engineering, Chinese Academy of Sciences, Beijing 100190, China; jueryi@126.com (E.J.); jjli@ipe.ac.cn (J.L.); wangzhuo@ipe.ac.cn (Z.A.W.); zhaomengyuan@ipe.ac.cn (M.Z.)
3 School of Chemical Engineering, University of Chinese Academy of Sciences, Beijing 100049, China
4 Gulbali Institute for Agriculture, Water and Environment, Charles Sturt University, Wagga Wagga, NSW 2678, Australia; biwang@csu.edu.au
* Correspondence: whqian@cc.tuat.ac.jp (E.W.Q.); ygdu@ipe.ac.cn (Y.D.)
† These authors contributed equally to this work.

Abstract

3′-sialyl-*N*-acetyllactosamine (3′-SLN) and 6′-sialyl-*N*-acetyllactosamine (6′-SLN) are two important human milk oligosaccharides (HMOs) which play significant functions in brain development and antiviral potential. However, their metabolism is still unknown. In this study, chemoenzymatically synthesized 3′-SLN and 6′-SLN were labeled with cyanine-7 (Cy7) via formation triazole (Tz) derivatives to investigate their metabolism and organ distribution in a mouse model. The fluorescence signals were detected in the brains of mice after 0.5 h of gavage with 3′-SLN-Tz-Cy7 and 6′-SLN-Tz-Cy7. It was found for the first time that both of them can cross the blood–brain barrier (BBB) as a whole and reach the brain in a sex-specific manner. And the results show that, whether in the in vivo imaging results or the brain fluorescence signal results, the male mice absorbed 3′-SLN-Tz-Cy7 more than 6′-SLN-Tz-Cy7; meanwhile, in the female mice, the results were exactly the opposite. Both 3′-SLN-Tz-Cy7 and 6′-SLN-Tz-Cy7 exhibited the highest fluorescence intensity in pulmonary tissues, followed by substantial hepatic deposition. This study would offer preliminary evidence for the hypothesis that the oral administration of 3′-SLN and 6′-SLN may promote brain development and provide a foundation for the further exploration of their functions in brain cognition.

Keywords: human milk oligosaccharides; 6′/3′-sialyl-*N*-acetyllactosamine; metabolism; blood-brain barrier; organ distribution

check for updates

Academic Editor: Giovanna Traina

Received: 29 October 2025
Revised: 27 November 2025
Accepted: 27 November 2025
Published: 2 December 2025

Citation: Jiao, R.; Ju, E.; Li, J.; Wang, Z.A.; Jiang, B.; Zhao, M.; Wang, B.; Qian, E.W.; Du, Y. Metabolism, Organ Distribution, and Blood-Brain Barrier Penetration of Human Milk Oligosaccharides—6′/3′-Sialyl-*N*-acetyllactosamine. *Appl. Sci.* **2025**, *15*, 12753. https://doi.org/10.3390/app152312753

Copyright: © 2025 by the authors. Licensee MDPI, Basel, Switzerland. This article is an open access article distributed under the terms and conditions of the Creative Commons Attribution (CC BY) license (https://creativecommons.org/licenses/by/4.0/).

1. Introduction

Sialic acid (Sia) [1], a class of nine-carbon acidic monosaccharides, is frequently localized at the termini of glycans on the cell surfaces and glycoconjugates. It is now known that Sia comprises a family of over 50 naturally occurring derivatives of the nine-carbon sugar neuraminic acid. Among them, *N*-acetylneuraminic acid (Neu5Ac, the C5 position is substituted with an *N*-acetyl group) is the most prevalent form, constituting the predominant sialic acid in humans [2–4]. Sia has various biological functions, such as modulation

of immune responses, interactions with pathogenic microorganisms, promotion of cell proliferation and differentiation, recognition, enhancement of neurodevelopment, facilitation of memory formation, and improvement of learning ability [5–8]. Deficiencies in sialylated level of glycoproteins and gangliosides in brains are associated with intellectual disabilities. Within the brain, Sia is predominantly localized to gangliosides, while polysialic acid—a homopolymer of sialic acid—resides on a limited number of glycoproteins [9]. Therefore, Sia is a conditionally essential nutrient during infancy and in human bodies [10,11]. These findings suggested importance of Sia during neonatal development. The de novo synthesis of Sia may be insufficient to meet the demands of all tissues in the rapidly growing infants, thereby necessitating an exogenous supply [12]. Importantly, though dietary supplementation of Sia promotes the production of gangliosides and neurotrophic factors [13], it has been observed that sialylated human milk oligosaccharides (SHMOs) are more easily absorbed and utilized than free Neu5Ac via oral administration [14,15], and significantly enhanced the learning ability of rats [16,17]. Therefore, it seems that external supplementation of SHMOs is more beneficial to the growth and development of brains than supplementation with free sialic acid.

3′-sialyl-*N*-acetyllactosamine (3′-SLN) and 6′-sialyl-*N*-acetyllactosamine (6′-SLN) are two significant SHMOs that are present in minimal quantities in human milk and are nearly undetectable [18]. However, their concentrations are much higher in bovine milk, with approximately 200 mg/kg for 6′-SLN in colostrum and 50 mg/kg for 3′-SLN in transitional milk [18,19]. Since the structures of 3′-SLN and 6′-SLN are generally present on the reducing ends of glycan chains of the human cells, especially in the airway, they can competitively block influenza virus binding to host receptors [20–24]. In 2021, Wang et al. [25] reported that sialylated milk oligosaccharides (SMOs) (including 3′-SL, 6′-SL, and 6′-SLN) can exert significant regulatory effects on key neurodevelopment-associated metabolites and neurotransmitter systems in piglet models. Notably, their findings demonstrate that the co-administration of SL (3′-SL and 6′-SL) with 6′-SLN (mixed in the sow milk replacer) synergistically enhanced neurochemical modulation compared to SL treatment alone, underscoring the potential of 6′-SLN to improve cerebral metabolic and synaptic signaling pathways. However, there is no direct evidence to support us in determining whether 6′-SLN enters the brains of piglets.

Until now, the metabolism and organ-specific distribution of orally administered 3′-SLN and 6′-SLN in mammals has remained unclear. Determining whether these compounds can cross the blood–brain barrier (BBB) is crucial for understanding their potential to influence cognitive function. In this study, cyanine7 (Cy7)-labeled 3′-SLN and 6′-SLN were synthesized to enable real-time, noninvasive in vivo imaging. Using this strategy, the biodistribution and metabolism of orally administered 3′-SLN and 6′-SLN were investigated in mice.

2. Materials and Methods

2.1. Materials

All chemicals utilized in this study were of analytical grade and procured from FUJIFILM Wako Pure Chemical Corporation (Osaka, Japan). GlcNAc-βproN$_3$ (3-azidopropyl-β-2-acetamido-2-deoxy-c-D-glucopyranoside) was purchased from Wuhan Glycogene Pharmaceutical Co., Ltd. (Wuhan, China). Sulfonated cyanine 7-alkyne (Cy7-alkyne) was obtained from New Research Sciences Co., Ltd. (Xi'an, China), and TLC Silica Gel 60 F254 was acquired from Sigma-Aldrich (Oakville, Canada). Streptomycin and isopropyl-β-D-thiogalactopyranoside (IPTG) were obtained from Solarbio (Beijing, China).

2.2. Synthesis, Purification, and Characterization of LacNAc-βproN$_3$, 6′-SLN-βproN$_3$, and 3′-SLN-βproN$_3$

According to the procedure of classical "copper-catalyzed azide–alkyne click chemistry (CuAAC)" [26], azide-substituted LacNAc, 3′-SLN, and 6′-SLN were first synthesized to obtain Cy7-labeled counterparts. The fluorescence spectrum (excitation wavelength, 745 nm; emission wavelength, 800 nm) of Cy7 provides better photon signal penetration through animal tissues because of the minimum tissue absorbance in the near-infrared (NIR) region (700–900 nm) [27]. In addition, it has been confirmed that the Cy7-labeled compounds can be effectively applied in animal in vivo imaging studies to investigate the metabolism and distribution of active substances [28,29].

The alkyne group on the Cy7 fluorophore can undergo the CuAAC reaction with the azide moiety within the oligosaccharides via formation triazole (Tz) derivatives, thereby forming a triazole linkage that covalently conjugates Cy7 with oligosaccharides. As described in the previous study [30], azide-substituted LacNAc (LacNAc-βproN$_3$) was enzymatically synthesized from Gal and GlcNAc-βproN$_3$. According to the protocol of a previous study [30], in order to obtain LacNAc-βproN$_3$ from Gal and GlcNAc-βproN$_3$, galactokinase (Galk), UDP–sugar pyrophosphorylase (USP), and β1,4-galactosyltransferase (β1,4-GalT) were used (Figure 1). LacNAc-βproN$_3$ was purified on the silica column (200 mesh). The column was eluted with a mobile phase consisting of ethyl acetate–methanol–water–acetic acid in a ratio of 4:2:1:0.2 (*v*/*v*/*v*/*v*). All fractions were detected by thin-layer chromatography (TLC). The fractions containing the target products were combined and concentrated using a rotary evaporator. According to the procedures we established for the enzymatic synthesis of 6′-SLN and 3′-SLN [23], azide-substituted 6′-SLN (6′-SLN-βproN$_3$) and 3′-SLN (3′-SLN-βproN$_3$) were synthesized from Neu5Ac and purified LacNAc-βproN$_3$ by employing CMP–sialic acid synthetase (CSS) plus α2,6-sialyltransferase (2,6ST) (Figure 1b) and CSS plus α2,3-sialyltransferase (2,3ST) (Figure 1c), respectively. Both were purified and characterized as described above. Finally, the purified product was characterized by LC-MS on a Thermo Scientific Dionex UltiMate 3000 LC system and a Single-Quadrupole Mass Spectrometer with an ESI ionization probe (Thermo Fisher Scientific, Waltham, MA, USA). The positive and negative modes were used to analyze LacNAc-βproN$_3$, 6′-SLN-βproN$_3$, and 3′-SLN-βproN$_3$ in the mass range of 200–1400 *m*/*z*. LacNAc-βproN$_3$: MS (ESI) *m*/*z* calculated for $C_{17}H_{29}ClN_4O_{11}^-$ [M + Cl]$^-$ 500.90, found 501.1 (Figure 2a). 6′-SLN-βproN$_3$: MS (ESI) *m*/*z* calculated for $C_{28}H_{46}N_5O_{19}^-$ [M − H]$^-$ 756.28, found 756.41 (Figure 2b). 3′-SLN-βproN$_3$: MS (ESI) *m*/*z* calculated for $C_{28}H_{46}N_5O_{19}^-$ [M − H]$^-$ 756.28, found 756.32 (Figure 2c).

2.3. Synthesis, Purification, and Characterization of LacNAc-Tz-Cy7, 6′-SLN-Tz-Cy7, and 3′-SLN-Tz-Cy7

According to the research of Presolski et al. [26], the CuAAC method was used to synthesize LacNAc-Tz-Cy7, 6′-SLN-Tz-Cy7, and 3′-SLN-Tz-Cy7 with slight modifications by increasing the concentration of vitamin C to 5 mM and replacing the ligand tris(3-hydroxypropyltriazolyl-methyl)amine (THTPA) with bis(1-(tert-butyl)-1H-1,2,3-triazol-4-yl) methyl (BTTAA).

Each reaction was carried out at the scale of 10 mL. The reaction was performed in the dark at room temperature, and the reaction vessel was sealed and stirred at a speed of 200 rpm to ensure the thorough mixing of all reactants throughout the reaction. The reaction was monitored using TLC.

To purify the Cy7-labeled oligosaccharides, the silica gel (200 mesh) purification method was employed. The procedures were the same as those described in Section 2.2. Cy7 and some impurities were first eluted out of column using a mobile phase of ethyl acetate–methanol–water–ammonia water at a ratio of 5:1:0.5:0.4 (*v*/*v*/*v*/*v*), followed by

eluting the product using a mobile phase of ethyl acetate–methanol–water–ammonia water at a ratio of 5:2:1:0.4 ($v/v/v/v$). After TLC detection, the product was collected, and the organic solvents were removed by rotary evaporation. The final product was analyzed by LC-MS. The LC-MS analysis was conducted using a state-of-the-art Thermo Scientific Dionex UltiMate 3000 LC system (Thermo Fisher Scientific, Waltham, MA, USA). This system was coupled with a Single-Quadrupole Mass Spectrometer equipped with an electrospray ionization (ESI) probe (Thermo Fisher Scientific, Waltham, MA, USA). The negative ion mode was specifically chosen for the detection of LacNAc-Tz-Cy7 (Figure 2d), 6′-SLN-Tz-Cy7 (Figure 2e) and 3′-SLN-Tz-Cy7 (Figure 2f). The analysis was performed within a mass range of 600 to 1600 m/z. LacNAc-Tz-Cy7: MS (ESI) m/z calculated for $C_{55}H_{74}N_7O_{18}S_2^-$ $[M-H]^-$ 1184.45317, found 1184.35951; MS (ESI) m/z calculated for $C_{55}H_{73}N_7O_{18}S_{22}^-$ $[(M-2H)/2]^-$ 591.72259, found 591.67575. 3′-SLN-Tz-Cy7: MS (ESI) m/z calculated for $C_{66}H_{91}N_8O_{26}S_2^-$ $[M-H]^-$ 1475.54859, found 1475.43165; MS (ESI) m/z calculated for $C_{66}H_{91}N_8O_{26}S_{22}^-$ $[(M–2H)/2]^-$ 737.27030, found 737.21295. 6′-SLN-Tz-Cy7: MS (ESI) m/z calculated for $C_{66}H_{91}N_8O_{26}S_2^-$ $[M-H]^-$ 1475.54859, found 1475.43401; MS (ESI) m/z calculated for $C_{66}H_{91}N_8O_{26}S_{22}^-$ $[(M-2H)/2]^-$ 737.27030, found 737.21163.

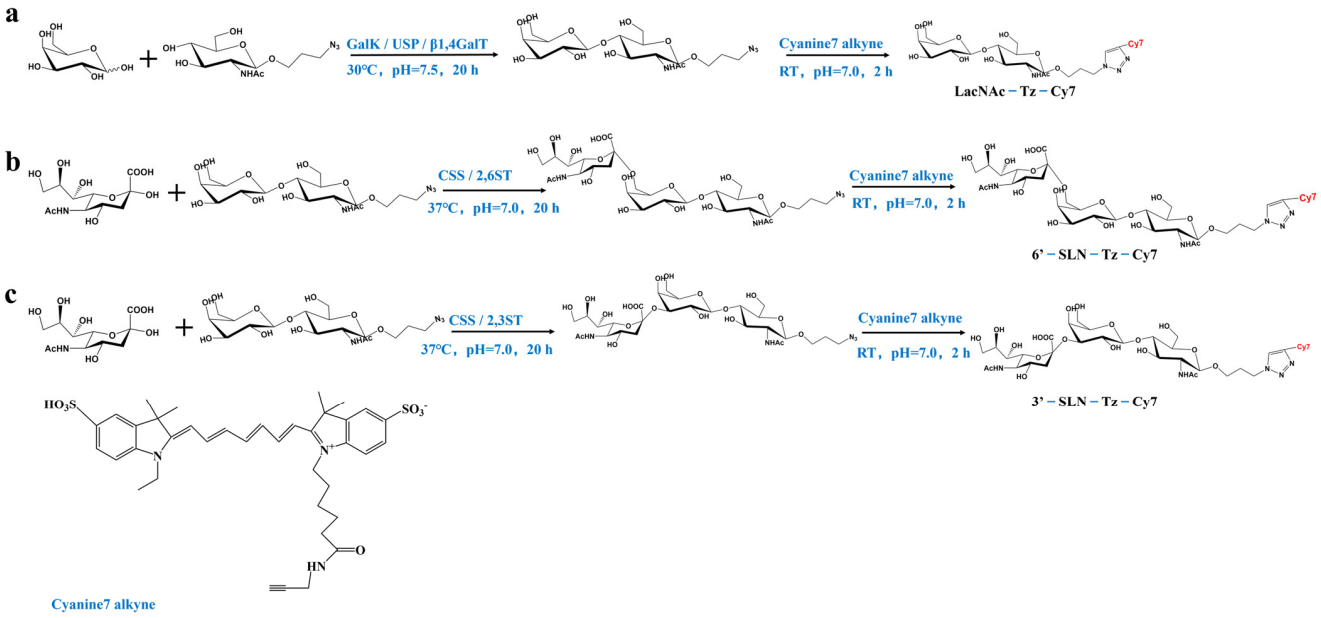


Figure 1. Chemoenzymatic synthesis of Cy7-labeled oligosaccharides. (**a**) The synthetic route of LacNAc-Tz-Cy7: LacNAc-βproN$_3$ was synthesized in the presence of GalK, USP, and β1,4-GalT at 30 °C, pH 7.5, and the reaction was finished after 20 h. LacNAc-Tz-Cy7 was synthesized in the presence of $CuSO_4$, BTTAA, and vitamin C at room temperature (RT), pH 7.0, and the reaction was finished after 2 h. (**b**) The synthetic route of 6′-SLN-Tz-Cy7: 6′-SLN-βproN$_3$ was synthesized in the presence of CSS and 2,6ST at 37 °C, pH 7.0, and the reaction was finished after 20 h. 6′-SLN-Tz-Cy7 was synthesized in the presence of $CuSO_4$, BTTAA, and vitamin C at room temperature, pH 7.0, and the reaction was finished after 2 h. (**c**) The synthetic route of 3′-SLN-Tz-Cy7: 3′-SLN-βproN$_3$ was synthesized in the presence of CSS and 2,3ST at 37 °C, pH 7.0, and the reaction was finished after 20 h. 3′-SLN-Tz-Cy7 was synthesized the presence of $CuSO_4$, BTTAA, and vitamin C at room temperature, pH 7.0, and the reaction was finished after 2 h; GalK, galactokinase; USP, UDP–sugar pyrophosphorylase; β1,4GalT, β1,4-galatosyltransferase; CSS, CMP–sialic acid synthetase; 2,6ST, α2,6-sialyltransferase; 2,3ST, α2,3-sialyltransferase: Cyanine 7 alkyne, sulfonated cyanine 7-alkyne. Tz, 1,2,3-triazole.

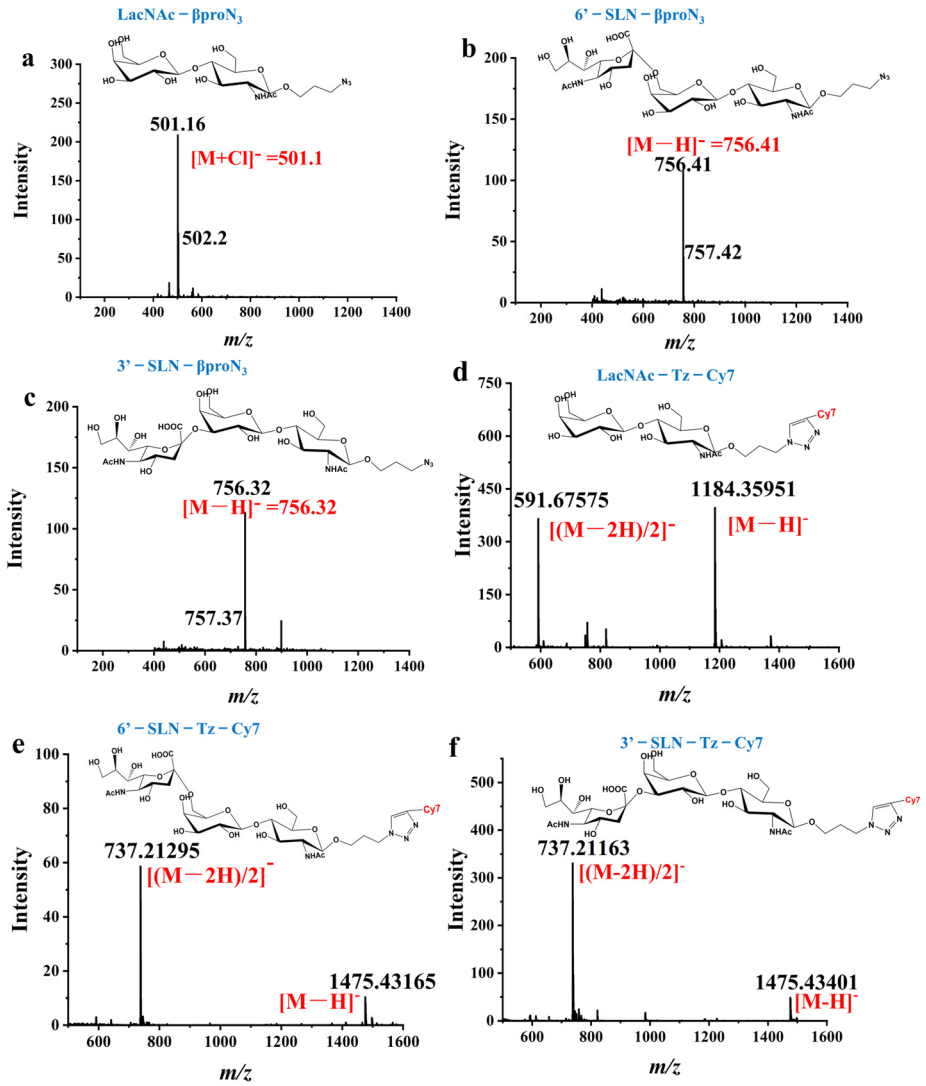


Figure 2. Characterization of purified azide-substituted oligosaccharides and Cy7-labeled oligosaccharides by LC-MS. (**a**) LacNAc-βproN$_3$, calculated m/z for $[M + Cl]^-$ was 500.90; (**b**) 6′-SLN-βproN$_3$, calculated m/z for $[M - H]^-$ was 756.28; (**c**) 3′-SLN-βproN$_3$, calculated m/z for $[M - H]^-$ was 756.28; (**d**) LacNAc-Tz-Cy7, calculated m/z for $[M - H]^-$ was 1184.45317, calculated m/z for $[(M - 2H)/2]^-$ was 591.72259; (**e**) 6′-SLN-Tz-Cy7, calculated m/z for $[M - H]^-$ was 1475.54859, calculated m/z for $[(M - 2H)/2]^-$ was 737.27030; (**f**) 3′-SLN-Tz-Cy7, calculated m/z for $[M - H]^-$ was 1475.54859, calculated m/z for $[(M - 2H)/2]^-$ was 737.27030.

2.4. Determination of the Optimal Concentration of Cy7-Labeled Oligosaccharides for In Vivo Imaging

All animals were acclimated under standard laboratory conditions (ventilated room, 25 ± 1 °C, 60 ± 5% humidity, 12 h light/dark cycle) and were given free access to standard water and food (SYXK-2024-0001). All procedures were conducted in accordance with the "Guiding Principles in the Care and Use of Animals" (China) and were approved by the Experimental Animal Ethics Committee of the Institute of Process Engineering, Chinese Academy of Sciences (IPEAECA2024046).

In order to investigate the optimal concentrations of Cy7-labeled oligosaccharides for imaging mouse organs, in vivo imaging studies on mice gavaged with different concentrations of Cy7 were initially conducted at various time points. The specific experimental procedures were described as follows. The in vivo imaging system used for the mice was IVIS Lumina XRMS Series III (Revvity, USA) with excitation filter of 745 nm and emission

filter of 800 nm. Images were acquired and analyzed on Live Image 3.1 software (Caliper Life Science, Hopkinton, MA, USA).

Five adult male C57BL/6J mice, aged between 17 and 20 weeks, were selected for the study. The purchased mice were raised in the mouse room for more than one week in advance to adapt to the environment. The conditions of mice raising were specified as follows: temperature, 25 ± 1 °C; relative humidity, 60%; ventilation and air exchange—air exchange rate, 15–20 times/h, air exchange rate within the cage, 30–100 times/h. To minimize inter-individual differences in metabolic conditions, the mice fasted for one day prior to the experiment. To reduce the interference of mouse fur on fluorescence intensity, the mice were shaved one day in advance. Subsequently, 100 μL of Cy7 solution at different concentrations (0, 100, 200, 300, and 600 μM) was administered via gavage. After gavage, the mice were anesthetized with isoflurane and imaged at 0.5, 1, 3, 6, and 12 h, respectively. Based on this, 300 μM Cy7 or Cy7-labeled oligosaccharides dissolved in water was selected for the following experiments in this study.

Unless otherwise specified, all mice, in vivo imaging instrumentation, and parameters in this study were maintained as described in this section.

2.5. Metabolism of LacNAc-Tz-Cy7, 6′-SLN-Tz-Cy7, and 3′-SLN-Tz-Cy7 by Real-Time In Vivo Imaging

To investigate metabolism of LacNAc-Tz-Cy7, 6′-SLN-Tz-Cy7, and 3′-SLN-Tz-Cy7 in vivo, eight adult C57BL/6J mice (17–20 weeks old) were allocated into four groups (n = 2 per group): the control group (two male mice), the LacNAc-Tz-Cy7 group (one male and one female), the 3′-SLN-Tz-Cy7 group (one male and one female), and the 6′-SLN-Tz-Cy7 group (one male and one female). Dorsal fur was depilated 24 h prior to imaging to minimize fluorescence interference. At the onset of experimentation, for the control group, each mouse received 100 μL saline and 100 μL 300 μM free Cy7 dye via oral gavage, respectively, while the LacNAc-Tz-Cy7, 3′-SLN-Tz-Cy7, and 6′-SLN-Tz-Cy7 groups were administered 100 μL of their respective 300 μM Cy7-conjugated compounds. In vivo fluorescence imaging was performed at 0.5, 1, 3, 6, and 12 h post-administration using an IVIS imaging system under standardized anesthesia (2% isoflurane/oxygen), with fluorescence signals captured at Cy7-specific wavelengths (excitation/emission: 745/800 nm). Image acquisition parameters, including exposure time and spatial resolution, were held constant across all time points. Signal intensities were quantified using Living Image™ software (version 4.8.2.20) [31]. Unless otherwise specified, all fluorescent imaging methods (including organ imaging mentioned hereafter) in this study were consistent with those described previously.

2.6. Metabolism and Organ Distribution of LacNAc-Tz-Cy7, 3′-SLN-Tz-Cy7, and 6′-SLN-Tz-Cy7 by Ex Vivo Fluorescence Imaging

A total of 32 C57BL/6J mice (22 male and 10 female, aged at 17–20 weeks) were allocated into six experimental groups. Group 1 comprised two adult male C57BL/6J mice that received 100 μL saline via oral gavage and immediately underwent cervical dislocation for baseline analysis. Groups 2–5 (six mice per group: 4 males + 2 female) underwent analysis procedures at sequential time points (0.5, 1, 3, 6, and 12 h post-gavage) for dissecting and imaging the organs. In each group, the first male mouse was administered 100 μL of 300 μM Cy7 as a time-matched control, while the remaining male and female mice received 100 μL of 300 μM LacNAc-Tz-Cy7, 3′-SLN-Tz-Cy7, and 6′-SLN-Tz-Cy7, respectively. Imaging conditions for organs were similar to those described in Section 2.5.

2.7. Detection of the Presence of 3′-SLN-Tz-Cy7 and 6′-SLN-Tz-Cy7 in Experimental Brains by MS

Following the ex vivo imaging experiments on mice, tissue samples were collected at multiple time points. To prove that the fluorescence signals in the brain tissue were caused by intact 3′-SLN-Tz-Cy7 and 6′-SLN-Tz-Cy7, the brain tissues of male mice 0.5 h after intragastric administration were selected for extraction and detection. The brain homogenate was extracted by methanol using a slightly modified protocol [32]. Specifically, 100 µL brain homogenate (300 mg/mL) was combined with 700 µL methanol in a centrifuge tube [32]. The mixture was vortexed for 10 min and centrifuged at 9000× *g* for 10 min at 10 °C. Then, 600 µL supernatant was transferred into a new Eppendorf tube for further analysis by LC-MS.

For LC-MS analysis, an Accela autosampler (Thermo Fisher Scientific, USA) was used in conjunction with an XAmide column (4.6 × 250 mm, 5 µm particle size; Acchrom, Wenling, China). A gradient elution system employing water and acetonitrile was applied (conditions: 70% acetonitrile + 30% water eluted for 45 min and flow rate was 0.7 mL/min), and the system was connected to an Exploris 480 mass spectrometer (detection limit: 50 fg) operated in negative ion mode (https://www.thermofisher.cn/order/catalog/product/cn/zh/BRE725533R (accessed on 13 November 2025)). The qualitative identification of 3′-SLN-Tz-Cy7 and 6′-SLN-Tz-Cy7 was achieved through selected ion monitoring (SIM), with specific precursor-to-product ion transitions monitored at *m*/*z* 1475.43274 and 1475.43274, respectively. Data acquisition was performed using Xcalibur software (version 3.0.63) from Thermo Fisher Scientific.

3. Results

3.1. Chemoenzymatic Synthesis and Characterization of LacNAc-Tz-Cy7, 3′-SLN-Tz-Cy7, and 6′-SLN-Tz-Cy7

Following previous studies [30], LacNAc-βproN$_3$ was first enzymatically synthesized from Gal and GlcNAc-βproN$_3$, which was further extended by 2,3ST and 2,6ST to produce 3′-SLN-βproN$_3$ and 6′-SLN-βproN$_3$, respectively (Figure 2a–c). Finally, LacNAc-Tz-Cy7 (Figure 2d), 6′-SLN-Tz-Cy7 (Figure 2e), and 3′-SLN-Tz-Cy7 (Figure 2f) were successfully obtained by the classical CuAAC method (Figure 1) [26]. All compounds were verified by MS and used in the following experiments.

3.2. Real-Time In Vivo Imaging of Oral Administrated LacNAc-Tz-Cy7, 6′-SLN-Tz-Cy7, and 3′-SLN-Tz-Cy7

Notably, mice administered with free Cy7 (the control group) exhibited rapid signal attenuation within the initial post-gavage 3 h, with nearly complete fluorescence signal loss by 6 h (Figure 3). Based on the analysis of the fluorescent intensity, it seems that there is only slight difference between 200 and 300 µM (Figure S1 in the Supplementary Materials). Thus, 300 µM Cy7 or Cy7-labeled oligosaccharides were chosen for the following experiments. Therefore, Cy7, LacNAc-Tz-Cy7, 6′-SLN-Tz-Cy7, and 3′-SLN-Tz-Cy7 at a concentration of 300 µM were administered to mice via gavage, respectively, and time-courses of their in vivo fluorescence imaging were investigated.

In the LacNAc-Tz-Cy7 group, sustained fluorescence signals were only observed in the gastrointestinal tract in the female group, suggesting a lower uptake of LacNAc-Tz-Cy7 in male mice than in female mice. And the fluorescence changes in the gastrointestinal tract for the 6′-SLN-Tz-Cy7 and 3′-SLN-Tz-Cy7 groups showed sex differences. As shown in Figure 3, the sex-based difference in the 6′-SLN-Cy7 group was less pronounced than that in the 3′-SLN-Cy7 group. The 6′-SLN-Tz-Cy7 and 3′-SLN-Tz-Cy7 groups exhibited sustained fluorescence signals in the gastrointestinal tract over 12 h (Figure 3). Notably, the fluorescence intensity in female mice administered with 3′-SLN-Tz-Cy7 was lower than

that of 6′-SLN-Tz-Cy7 at the same time points. Moreover, in female mice, a pronounced fluorescence decrease in the 3′-SLN-Tz-Cy7 group was observed 3 h post-gavage, suggesting rapid metabolism or fluorescence quenching during 3 h. In contrast, in male mice administered with 6′-SLN-Tz-Cy7, the fluorescence intensity exhibited a gradual declined over time, while no substantial fluorescence reduction in the 3′-SLN-Tz-Cy7 group was detected until 12 h post-administration. Absorption and metabolism of LacNAc-Tz-Cy7 also exhibited markedly sex-specific differences. Specifically, fluorescence intensity in female mice remained consistently stronger than that in males throughout 12 h. A significant fluorescence attenuation in the LacNAc-Tz-Cy7 group was observed in both sexes after 3 h of administration of LacNAc-Tz-Cy7. However, by 12 h, the fluorescence signal in male mice had nearly vanished, whereas detectable signals remained in females.

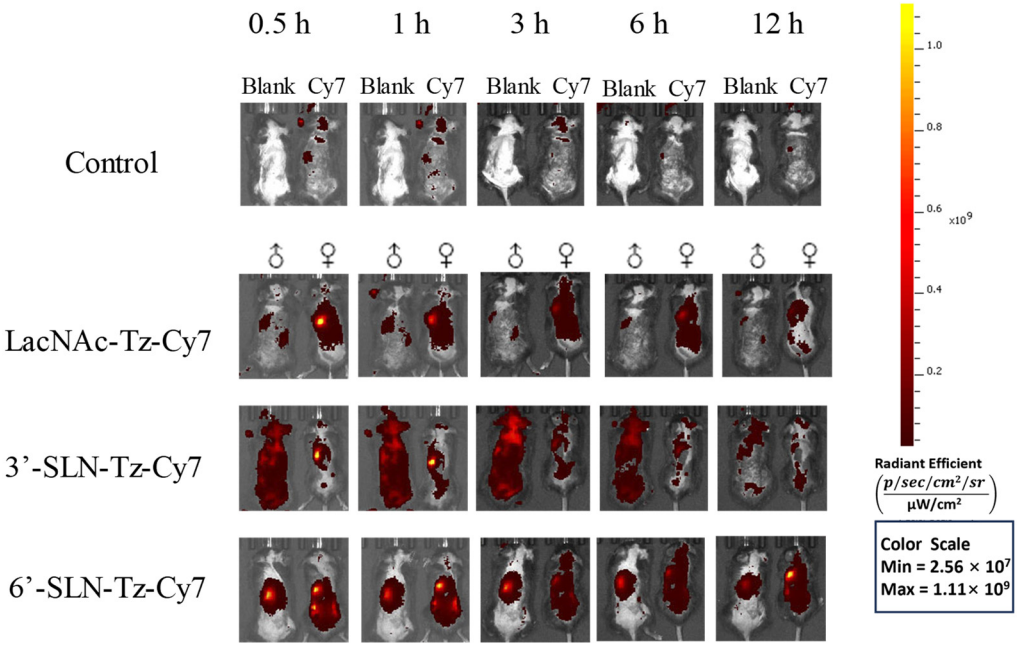


Figure 3. Time-courses of in vivo fluorescence imaging of gavaged mice. The mice were imaged after 100 µL of 300 µM LacNAc-Tz-Cy7, 3′-SLN-Tz-Cy7, and 6′-SLN-Tz-Cy7 intragastrically applied, respectively. Blank: fluorescence changes in the male mice after intragastric administration of 100 µL of physiological saline; Cy7: fluorescence changes in the male mice after intragastric administration of 100 µL of 300 µM Cy7; ♂: fluorescence changes in male mice after intragastric administration of 100 µL of 300 µM Cy7-labeled oligosaccharides; ♀: fluorescence changes in female mice after intragastric administration of 100 µL of 300 µM Cy7-labeled oligosaccharides.

3.3. Organ Distribution of Cy7-Labeled Oligosaccharides by Ex Vivo Imaging

As shown in Figure 4, no fluorescence signals were detected in the brains of the Cy7 group for 12 h. As shown in Figure 4a,c, the fluorescence signals were detected in brains of mice dealt with 3′-SLN-Tz-Cy7 at 0.5 h post-intragastric administration, and signals were observed in brains of both male and female mice. The fluorescence signals in brains of male mice administered with 3′-SLN-Tz-Cy7 disappeared by 3 h post-administration, while in female mice, the signals were undetectable as early as 1 h post-administration. On the other hand, fluorescence was detected in the brains of the 6′-SLN-Tz-Cy7 group after 0.5 h of gavage; as shown in Figure 4a,d, fluorescence signals were detected in the brains after 0.5 h of gavage of 6′-SLN-Tz-Cy7. Fluorescence intensity was strongest in male mouse brains 0.5 h post-administration of 6′-SLN-Tz-Cy7 but strongest after 1 h of administration in female mice. As illustrated in Figure 4a,b, fluorescence signals were detected in the brain tissue of mice 0.5 h post-gavage of LacNAc-Tz-Cy7, and persisted 3 h post-gavage.

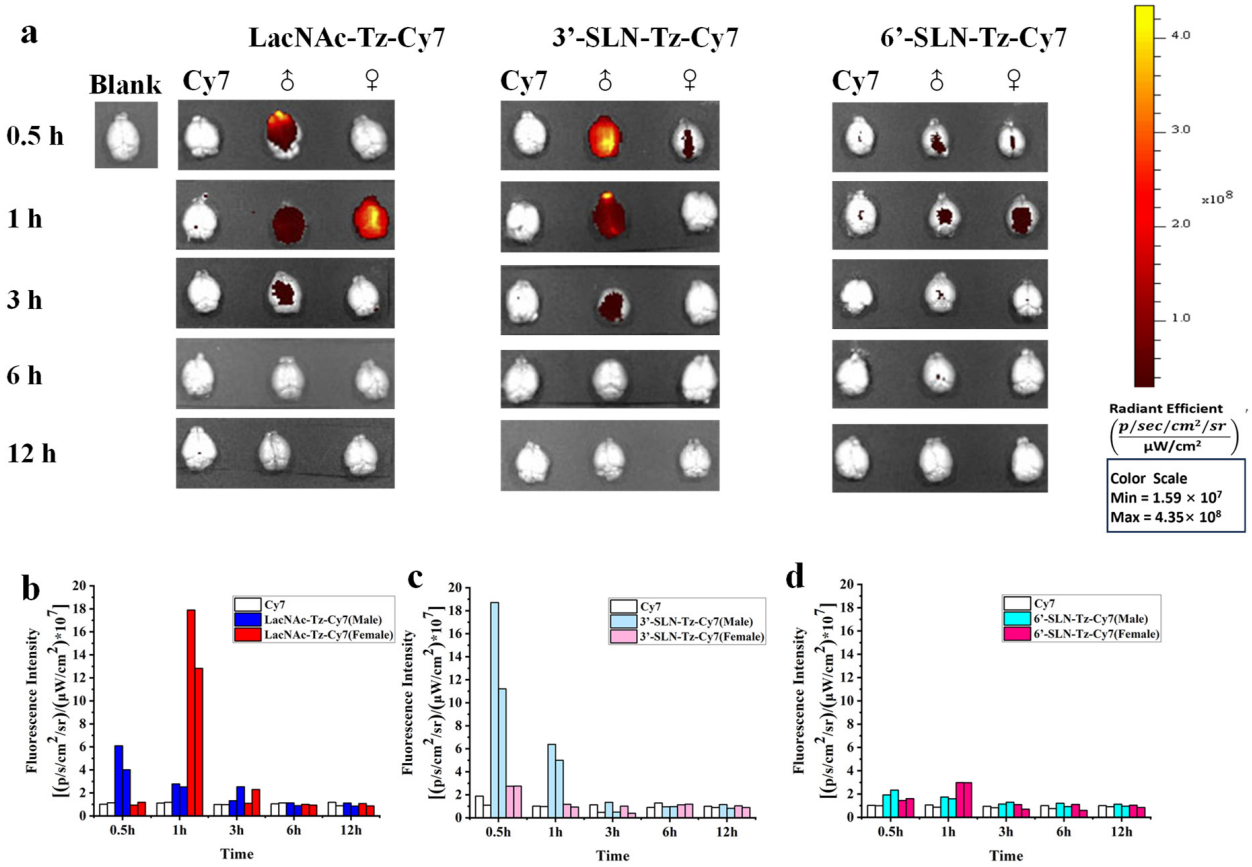


Figure 4. The fluorescence changes in brains of C57BL/6J adult mice following the administration of LacNAc-Tz-Cy7, 3′-SLN-Tz-Cy7, and 6′-SLN-Tz-Cy7 at different time points. (**a**) Blank: fluorescence changes in the brain of male mice after intragastric administration of 100 μL of physiological saline; Cy7: fluorescence changes in brains of male mice after intragastric administration of 100 μL of 300 μM Cy7; ♂: fluorescence changes in brains of male mice after intragastric administration of 100 μL of 300 μM Cy7-labeled oligosaccharides; ♀: fluorescence changes in brains of female mice after intragastric administration of 100 μL of 300 μM Cy7-labeled oligosaccharides. Note: This study included two parallel experiments, with images from the additional parallel group presented in the Supplementary Materials Figure S2a–c. (**b**) Comparison of the fluorescence changes in brains of C57BL/6J adult male and female mice following the administration of Cy7 and LacNAc-Tz-Cy7 (Bars of the same color represent results from two parallel experiments); (**c**) comparison of the fluorescence changes in brains of C57BL/6J adult male and female mice following the administration of Cy7 and 3′-SLN-Tz-Cy7 (bars of the same color represent results from two parallel experiments); (**d**) comparison of the fluorescence changes in brains of C57BL/6J adult male and female mice following the administration of Cy7 and 6′-SLN-Tz-Cy7 (bars of the same color represent results from two parallel experiments).

The strongest fluorescence intensity was observed in pulmonary tissues, followed by liver. Moderate fluorescence accumulation was observed in the kidneys, while only trace amounts of fluorescence signals were detected in the hearts and spleens (Figure 5).

3.4. Determining the Presence of 6′-SLN-Tz-Cy7 and 3′-SLN-Tz-Cy7 in Experimental Brains by LC-MS

Utilizing LC-MS direct detection of 6′-SLN-Tz-Cy7 and 3′-SLN-Tz-Cy7 was conducted in brains of experimental mice after 0.5 h of gavage, respectively. It was observed that the complete structures of 6′-SLN-Tz-Cy7 (Figure 6a) and 3′-SLN-Tz-Cy7 (Figure 6b) were indeed identified in the brains of experimental mice, respectively.

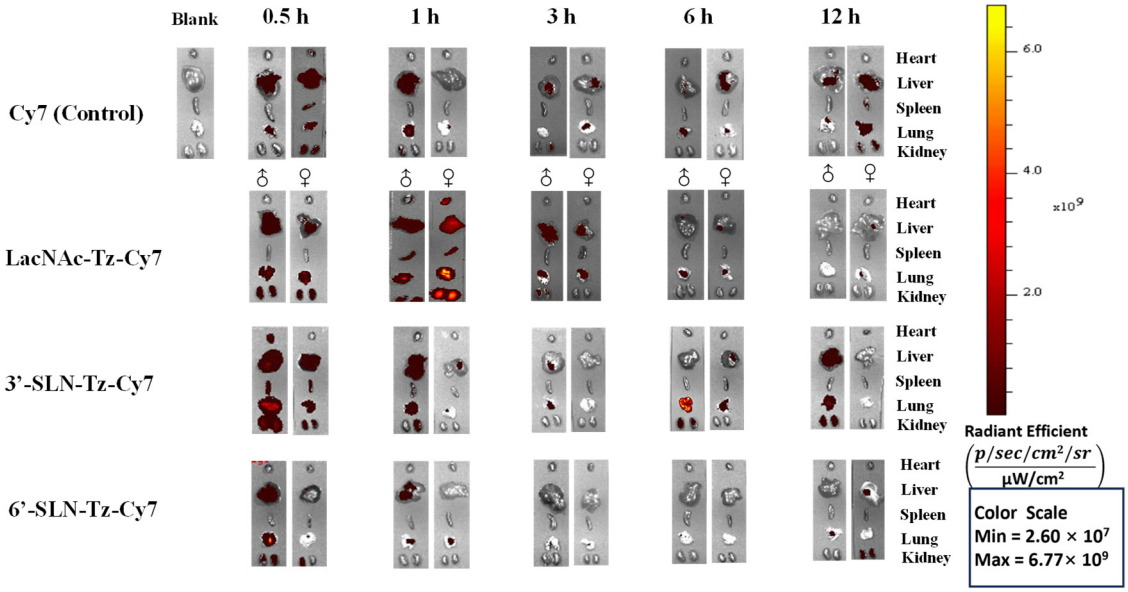


Figure 5. The fluorescence changes in different organs of C57BL/6J adult mice. LacNAc-Tz-Cy7, 3′-SLN-Tz-Cy7, and 6′-SLN-Tz-Cy7 indicated mice were dissected following the administration of 100 μL 300 μM LacNAc-Tz-Cy7, 3′-SLN-Tz-Cy7, and 6′-SLN-Tz-Cy7 at different time points. Blank: fluorescence changes in the organs of male mice after intragastric administration of 100 μL of physiological saline; Cy7: fluorescence changes in organs of male mice after intragastric administration of 100 μL of 300 μM Cy7; ♂: fluorescence changes in organs of male mice after intragastric administration of 100 μL of 300 μM Cy7-labeled oligosaccharides; ♀: fluorescence changes in brains of female mice after intragastric administration of 100 μL of 300 μM Cy7-labeled oligosaccharides.

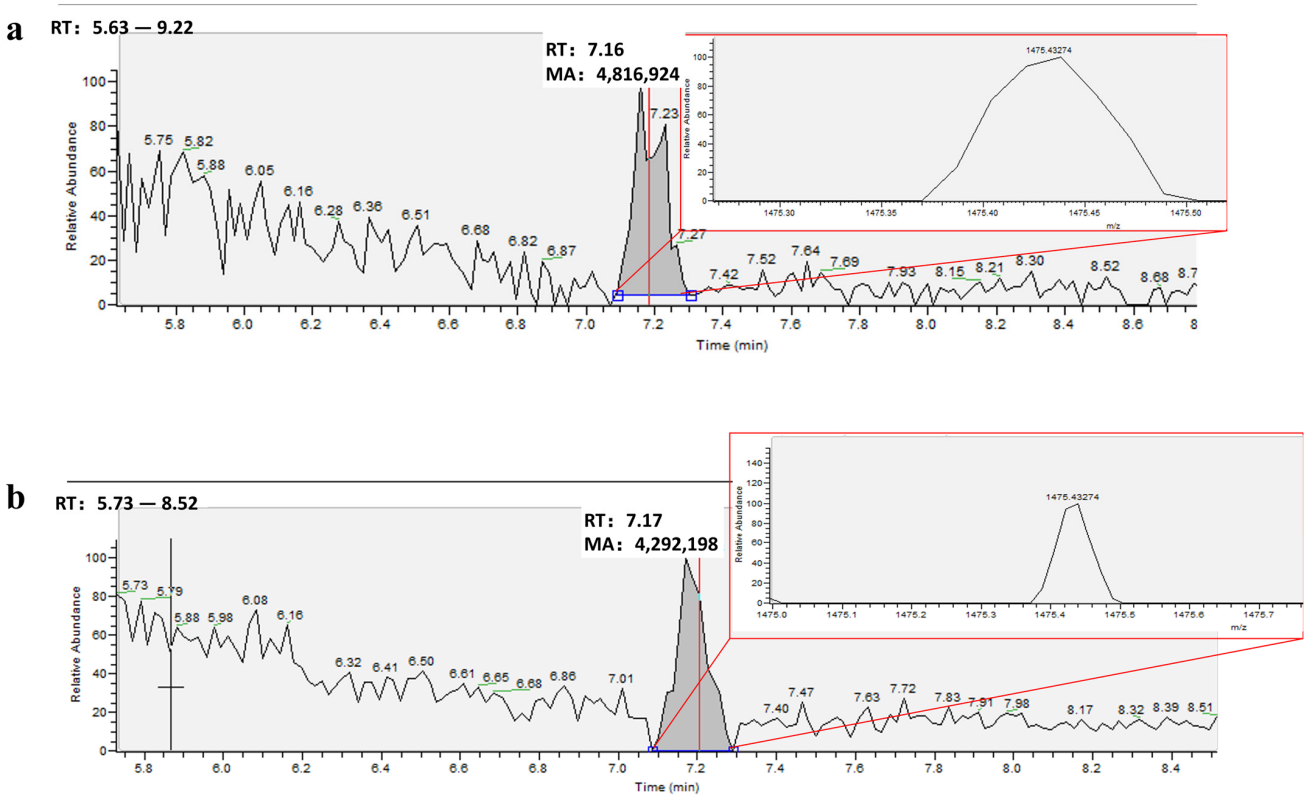


Figure 6. Detecting the presence of 6′-SLN-Tz-Cy7 (**a**) and 3′-SLN-Tz-Cy7 (**b**) in experimental brains (0.5 h after oral administration in male mice) by LC-MS.

4. Discussion

In this study, Cy7-labeled LacNAc, 3′-SLN and 6′-SLN were successfully synthesized by the chemoenzymatic approach. Their metabolism and distribution were investigated and compared. It was observed that 3′-SLN-Tz-Cy7 and 6′-SLN-Tz-Cy7 can cross the BBB and reach the brain as a whole. As far as we know, this is the first report employing fluorescently labeled HMOs to directly visualize and evaluate their metabolic fate and organ distribution in vivo.

In Figure 3, the observations suggested minimal systemic absorption or metabolic retention of free Cy7, confirming that it can be utilized as a transient tracer. And the comparation of the in vivo fluorescence imaging results preliminarily demonstrated potential sex-dependent differences in metabolism of 6′-SLN, 3′-SLN, and LacNAc as well as metabolic differences among them. However, the exact mechanism(s) underlying the metabolic differences need(s) further study.

Metabolism and organ distribution of Cy7 and Cy7-labeled oligosaccharides were further assessed by ex vivo imaging. The results in Figure 4 suggested that Cy7 alone could not cross the BBB. The fluorescence signals detected in brains of mice fed with 3′-SLN-Tz-Cy7 indicated that either a lower uptake or a faster metabolism of 3′-SLN-Tz-Cy7 in female brains than in male brains. Meanwhile, in the 6′-SLN-Tz-Cy7 group, a slightly faster metabolic rate or clearance of 6′-SLN-Tz-Cy7 in male brains than that of females. This sex-specific pattern contrasted with the metabolic dynamics of 3′-SLN-Tz-Cy7 in the brain. In the group of LacNAc-Tz-Cy7, the sex-specific also be observed.

Imaging data for other organs were presented in Figure 5, revealing organ-specific distribution profiles of fluorescence signals for mice treated with LacNAc-Tz-Cy7, 3′-SLN-Tz-Cy7, and 6′-SLN-Tz-Cy7. The pronounced pulmonary retention may reflect structural affinity for lung-specific vascular or epithelial receptors, though the exact mechanisms remain to be elucidated.

As illustrated in Figure 4a, notable fluorescence signals in the experimental brains from the 6′-SLN-Tz-Cy7 and 3′-SLN-Tz-Cy7 groups were observed. Notwithstanding, they did not conclusively confirm that both 6′-SLN and 3′-SLN crossed the BBB as a whole. In Figure 6, the complete structures of 6′-SLN-Tz-Cy7 and 3′-SLN-Tz-Cy7 were identified in the brains, which indicated that 6′-SLN-Tz-Cy7 and 3′-SLN-Tz-Cy7 can pass through the BBB and be absorbed by the brain in their complete structural forms. Since it was found that Cy7 alone could not cross the BBB and reach the brain, the above results suggested that 6′-SLN and 3′-SLN could cross the BBB.

Previous studies [15,33,34] have explored the absorption and metabolism of free Neu5Ac and found that exogenously administered Neu5Ac and SHMOs (3′-SL and 6′-SL) can cross the BBB and reach the brain via oral administration. However, it has remained unclear whether administered 3′-SLN and 6′-SLN could pass through the BBB, because no direct evidence has been obtained for the presence of the whole structure of SL in brain tissues [15,33,35]. However, in these previously reported studies, ^{14}C- or ^{13}C-labeled 3′-SL and 6′-SL administered orally or by intravenous injection was employed to track their organ distribution and metabolic status, and detection of the labeled isotopes in metabolites and organs does not necessarily imply the presence of complete structure of 3′-SL or 6′-SL. Noticeably, the current study presented the first direct evidence supporting the observation that orally administered 3′-SLN and 6′-SLN can cross BBB and enter brain. Therefore, this study lays the foundation for future study towards their function in promoting brain development and enhancing cognitive abilities.

It is worth pointing out that future experiments (e.g., with a larger number of animals and functional tests of cognitive effects of 3′-SLN and 6′-SLN) need to be performed.

In addition, although fluorescent labeling offers the advantage of in vivo imaging, easy quenching and the relatively high cost of fluorescent reagents present some limitations.

5. Conclusions

Cy7-labeled LacNAc, 3′-SLN, and 6′-SLN were successfully synthesized via a chemoenzymatic approach. Their in vivo metabolism and biodistribution were subsequently investigated and compared. For the first time, it was observed that both 3′-SLN-Tz-Cy7 and 6′-SLN-Tz-Cy7 can cross the BBB and reach the brain in intact forms. To the best of our knowledge, this preliminary study constitutes the first report utilizing fluorescently labeled HMOs to directly visualize and assess their metabolic fate and organ distribution in vivo. The current strategy would be potentially used to investigate metabolism and organ distribution of other functional oligosaccharides.

Supplementary Materials: The following supporting information can be downloaded at: https://www.mdpi.com/article/10.3390/app152312753/s1, Figure S1: Time course of in vivo fluorescence imaging after different concentrations of Cy7 were administered to 17–20 week-old male C57BL/6J mice; Figure S2: The parallel experiments' results of fluorescence changes in organs of C57BL/6J adult mice following the administration of LacNAc-Tz-Cy7, 3′-SLN-Tz-Cy7, and 6′-SLN-Tz-Cy7 at different time points.

Author Contributions: Writing—original draft preparation, investigation and methodology, R.J.; investigation and methodology, E.J.; funding acquisition, Z.A.W.; investigation, B.J.; investigation, M.Z.; investigation, B.W.; data curation and writing—review and editing, J.L.; conceptualization, Y.D.; supervision, E.W.Q. All authors have read and agreed to the published version of the manuscript.

Funding: This research was funded by the National Key R&D Program of China (No. 2023YFC2308000).

Institutional Review Board Statement: All the animals were acclimated under standard laboratory conditions (ventilated room, 25 ± 1 °C, 60 ± 5% humidity, 12 h light/dark cycle) and had free access to standard water and food (SYXK-2024-0001). All procedures were conducted in accordance with the "Guiding Principles in the Care and Use of Animals" (China) and were approved by the Experimental Animal Ethics Committee of the Institute of Process Engineering, Chinese Academy of Sciences (IPEAECA2024046).

Data Availability Statement: The datasets generated during and/or analysed during the current study are available from the corresponding author on reasonable request.

Conflicts of Interest: The authors declare no conflicts of interest.

Abbreviations

The following abbreviations are used in this manuscript:

3′-SLN	3′-sialyl-*N*-acetyllactosamine
6′-SLN	6′-sialyl-*N*-acetyllactosamine
HMOs	human milk oligosaccharides
Cy7	Cyanine-7
BBB	blood–brain barrier
Sia	sialic acid
Neu5Ac	*N*-acetylneuraminic acid
SL	sialyllactose
IPTG	Isopropyl-β-D-thiogalactopyranoside
CuAAC	Copper-catalyzed azide–alkyne click chemistry
TLC	Thin-layer chromatography
BTTAA	Bis(1-(tert-butyl)-1H-1,2,3-triazol-4-yl) methyl
SIM	Selected ion monitoring

References

1. Blix, F.G.; Gottschalk, A.; Klenk, E. Proposed nomenclature in the field of neuraminic and sialic acids. *Nature* **1957**, *179*, 1088. [CrossRef] [PubMed]
2. Schauer, R.; Kamerling, J.P. Exploration of the Sialic Acid World. *Adv. Carbohydr. Chem. Biochem.* **2018**, *75*, 1–213. [CrossRef]
3. Liu, F.; Simpson, A.B.; D'Costa, E.; Bunn, F.S.; van Leeuwen, S.S. Sialic acid, the secret gift for the brain. *Crit. Rev. Food Sci.* **2022**, *63*, 9875–9894. [CrossRef] [PubMed]
4. Schauer, R.; Kamerling, J.P. Chemistry, biochemistry and biology of sialic acids. In *Glycoproteins II*; Elsevier Science: Amsterdam, The Netherlands, 1997; pp. 243–402. [CrossRef]
5. Oetke, C.; Vinson, M.C.; Jones, C.; Crocker, P.R. Sialoadhesin-deficient mice exhibit subtle changes in B- and T-cell populations and reduced immunoglobulin M levels. *Mol. Cell. Biol.* **2006**, *26*, 1549–1557. [CrossRef] [PubMed]
6. Yamada, S.; Suzuki, Y.; Suzuki, T.; Le, M.Q.; Nidom, C.A.; Sakai-Tagawa, Y.; Muramoto, Y.; Ito, M.; Kiso, M.; Horimoto, T.; et al. Haemagglutinin mutations responsible for the binding of H5N1 influenza A viruses to human-type receptors. *Nature* **2006**, *444*, 378–382. [CrossRef]
7. Salvolini, E.; Di Giorgio, R.; Curatola, A.; Mazzanti, L.; Fratto, G. Biochemical modifications of human whole saliva induced by pregnancy. *BJOG Int. J. Obstet. Gynaecol.* **2005**, *105*, 656–660. [CrossRef]
8. Chinta, S.; Sonali, L.; Pavithra, R.; Drisya Raj, M.P.; Kanimozhi, N.V.; Sukumar, M. Dietary glycans and their role in human health: Implications for gut health, metabolism, and functional foods. *Glycosci. Ther.* **2025**, *1*, 100004. [CrossRef]
9. Zhang, Z.; Liang, R.; Hooijschuur, K.C.; de Vries, R.P.; Li, Z.; Boons, G.J. Chemoenzymatically Synthesized O-Acetylated GD3 Gangliosides to Examine Viral Receptor Specificities in a Cellular Context. *Angew. Chem. Int. Ed.* **2025**, *13*, 179–189. [CrossRef]
10. Schnaar, R.L.; Gerardy-Schahn, R.; Hildebrandt, H. Sialic Acids in the Brain: Gangliosides and Polysialic Acid in Nervous System Development, Stability, Disease, and Regeneration. *Physiol. Rev.* **2014**, *94*, 461–518. [CrossRef]
11. Xu, J.; Song, J.; Xu, H. Structural diversity, composition variation and neurodevelopmental-promoting effects of human milk oligosaccharides: A systematic review. *Carbohydr. Polym.* **2025**, *368 Pt 2*, 124229. [CrossRef]
12. Bardor, M.; Nguyen, D.H.; Diaz, S.; Varki, A. Mechanism of Uptake and Incorporation of the Non-human Sialic Acid N-Glycolylneuraminic Acid into Human Cells. *J. Biol. Chem.* **2005**, *280*, 4228–4237. [CrossRef] [PubMed]
13. Skaper, S.D.; Leon, A.; Toffano, G. Ganglioside function in the development and repair of the nervous system. From basic science to clinical application. *Mol. Neurobiol.* **1989**, *3*, 173–199. [CrossRef]
14. Chen, X. Human Milk Oligosaccharides (HMOS): Structure, Function, and Enzyme-Catalyzed Synthesis. *Adv. Carbohydr. Chem. Biochem.* **2015**, *72*, 113–190. [CrossRef] [PubMed]
15. Witt, W.; von Nicolai, H.; Zilliken, F. Uptake and distribution of orally applied N-acetyl-(14C)neuraminosyl-lactose and N-acetyl-(14C)neuraminic acid in the organs of newborn rats. *Nutr. Metab.* **1979**, *23*, 51–61. [CrossRef]
16. Sakai, F.; Ikeuchi, Y.; Urashima, T.; Fujihara, M.; Ohtsuki, K.; Yanahira, S. Effects of Feeding Sialyllactose and Galactosylated *N*-Acetylneuraminic Acid on Swimming Learning Ability and Brain Lipid Composition in Adult Rats. *J. Appl. Glyosci.* **2006**, *53*, 249–254. [CrossRef]
17. Oliveros, E.; Vazquez, E.; Barranco, A.; Ramirez, M.; Gruart, A.; Delgado-Garcia, J.M.; Buck, R.; Rueda, R.; Martin, M.J. Sialic Acid and Sialylated Oligosaccharide Supplementation during Lactation Improves Learning and Memory in Rats. *Nutrients* **2018**, *10*, 1519. [CrossRef]
18. van Leeuwen, S.S.; Te Poele, E.M.; Chatziioannou, A.C.; Benjamins, E.; Haandrikman, A.; Dijkhuizen, L. Goat Milk Oligosaccharides: Their Diversity, Quantity, and Functional Properties in Comparison to Human Milk Oligosaccharides. *J. Agric. Food Chem.* **2020**, *68*, 13469–13485. [CrossRef]
19. Martin-Sosa, S.; Martin, M.J.; Garcia-Pardo, L.A.; Hueso, P. Sialyloligosaccharides in human and bovine milk and in infant formulas: Variations with the progression of lactation. *J. Dairy Sci.* **2003**, *86*, 52–59. [CrossRef]
20. Atack, J.M.; Day, C.J.; Poole, J.; Brockman, K.L.; Timms, J.R.L.; Winter, L.E.; Haselhorst, T.; Bakaletz, L.O.; Barenkamp, S.J.; Jennings, M.P. The Nontypeable Haemophilus influenzae Major Adhesin Hia Is a Dual-Function Lectin That Binds to Human-Specific Respiratory Tract Sialic Acid Glycan Receptors. *mBio* **2020**, *11*, 6. [CrossRef]
21. Kocabiyik, O.; Cagno, V.; Silva, P.J.; Zhu, Y.; Sedano, L.; Bhide, Y.; Mettier, J.; Medaglia, C.; Da Costa, B.; Constant, S.; et al. Non-Toxic Virucidal Macromolecules Show High Efficacy Against Influenza Virus Ex Vivo and In Vivo. *Adv. Sci.* **2021**, *8*, 2001–2012. [CrossRef] [PubMed]
22. Shinya, K.; Ebina, M.; Yamada, S.; Ono, M.; Kasai, N.; Kawaoka, Y. Influenza virus receptors in the human airway. *Nature* **2006**, *440*, 435–436. [CrossRef]
23. Zhu, Y.; Sysoev, A.A.; Silva, P.H.J.; Batista, M.; Stellacci, F. Antiviral Mechanism of Virucidal Sialic Acid Modified Cyclodextrin. *Pharmaceutics* **2023**, *15*, 582. [CrossRef]
24. Chu, X.; Yin, X.; Tian, Y.; Jiang, W.; Zhao, Z.; Wang, J.; Cao, X.; Sang, J.; Xie, Q.; Li, T.; et al. Characterizations of a novel triple-reassortant H3N3 avian influenza A virus isolated from chickens in China. *Poult. Sci.* **2025**, *104*, 106–148. [CrossRef]

25. Wang, H.X.; Chen, Y.; Haque, Z.; de Veer, M.; Egan, G.; Wang, B. Sialylated milk oligosaccharides alter neurotransmitters and brain metabolites in piglets: An In vivo magnetic resonance spectroscopic (MRS) study. *Nutr. Neurosci.* **2021**, *24*, 885–895. [CrossRef]
26. Presolski, S.I.; Hong, V.P.; Finn, M.G. Copper-Catalyzed Azide-Alkyne Click Chemistry for Bioconjugation. *Curr. Protoc. Chem. Biol.* **2011**, *3*, 153–162. [CrossRef]
27. Frangioni, J. In vivo near-infrared fluorescence imaging. *Curr. Opin. Chem. Biol.* **2003**, *7*, 626–634. [CrossRef] [PubMed]
28. Xiao, L.; Zhang, Y.; Liu, Z.; Yang, M.; Pu, L.; Pan, D. Synthesis of the Cyanine 7 labeled neutrophil-specific agents for noninvasive near infrared fluorescence imaging. *Bioorg. Med. Chem. Lett.* **2010**, *20*, 3515–3517. [CrossRef]
29. Zhang, C.; Ling, X.; Guo, Y.; Yuan, C.; Cheng, H.; Ye, X.; Ma, R.; Zhang, Y.; Li, Y.; Chang, X.; et al. Evaluation of COC183B2 antibody targeting ovarian cancer by near-infrared fluorescence imaging. *Chin. J. Cancer Res.* **2019**, *31*, 673–685. [CrossRef] [PubMed]
30. Jiao, R.; Zhang, L.; You, R.; Peng, X.; Pei, C.; Jiang, B.; Hu, M.; Li, J.; Du, Y.; Qian, E.W. Efficient and Cost-Effective Synthesis of N-Acetyllactosamine by Sequential Modular Enzymatic Cascade Reactions Involving NTP Regeneration. *J. Agric. Food Chem.* **2024**, *76*, 28060–28071. [CrossRef] [PubMed]
31. Freeberg, M.A.T.; Farhat, Y.M.; Easa, A.; Kallenbach, J.G.; Malcolm, D.W.; Buckley, M.R.; Benoit, D.S.W.; Awad, H.A. Serpine1 Knockdown Enhances MMP Activity after Flexor Tendon Injury in Mice: Implications for Adhesions Therapy. *Sci. Rep.* **2018**, *8*, 5810. [CrossRef]
32. Jang, S.-I.; Eom, H.Y.; Hwang, J.H.; Kim, L.; Lee, J.-H. Simultaneous Quantification of 3′- and 6′-Sialyllactose in Rat Plasma Using Liquid Chromatography-Tandem Mass Spectrometry and Its Application to a Pharmacokinetic Study. *Molecules* **2021**, *26*, 1177. [CrossRef] [PubMed]
33. Nohle, U.; Schauer, R. Metabolism of sialic acids from exogenously administered sialyllactose and mucin in mouse and rat. *Hoppe Seylers Z. Physiol. Chem.* **1984**, *365*, 1457–1467. [CrossRef]
34. Eckhardt, M.; Bukalo, O.; Chazal, G.; Wang, L.; Goridis, C.; Schachner, M.; Gerardy-Schahn, R.; Cremer, H.; Dityatev, A. Mice Deficient in the Polysialyltransferase ST8SiaIV/PST-1 Allow Discrimination of the Roles of Neural Cell Adhesion Molecule Protein and Polysialic Acid in Neural Development and Synaptic Plasticity. *J. Neurosci.* **2000**, *20*, 5234–5244. [CrossRef]
35. Galuska, C.E.; Rudloff, S.; Kuntz, S.; Borsch, C.; Reutzel, M.; Eckert, G.; Galuska, S.P.; Kunz, C. Metabolic fate and organ distribution of 13C-3′-sialyllactose and 13C-N-acetylneuraminic acid in wild-type mice—No evidence for direct incorporation into the brain. *J. Funct. Foods* **2020**, *75*, 104268. [CrossRef]

Disclaimer/Publisher's Note: The statements, opinions and data contained in all publications are solely those of the individual author(s) and contributor(s) and not of MDPI and/or the editor(s). MDPI and/or the editor(s) disclaim responsibility for any injury to people or property resulting from any ideas, methods, instructions or products referred to in the content.